Cell, Vol. 120, 137–149, January 14, 2005, Copyright ©2005 by Elsevier Inc. DOI 10.1016/j.cell.2004.11.012

GSK-3β Regulates Phosphorylation of CRMP-2 and Neuronal Polarity

Takeshi Yoshimura,[1] Yoji Kawano,[1] Nariko Arimura,[1] Saeko Kawabata,[1] Akira Kikuchi,[2] and Kozo Kaibuchi[1,*]
[1]Department of Cell Pharmacology
Graduate School of Medicine
Nagoya University
65 Tsurumai, Showa-ku, Nagoya
Aichi 466-8550
[2]Department of Biochemistry
Graduate School of Biomedical Sciences
Hiroshima University
1-2-3, Kasumi, Minami-ku
Hiroshima 734-8551
Japan

Summary

Neurons are highly polarized and comprised of two structurally and functionally distinct parts, an axon and dendrites. We previously showed that collapsin response mediator protein-2 (CRMP-2) is critical for specifying axon/dendrite fate, possibly by promoting neurite elongation via microtubule assembly. Here, we showed that glycogen synthase kinase-3β (GSK-3β) phosphorylated CRMP-2 at Thr-514 and inactivated it. The expression of the nonphosphorylated form of CRMP-2 or inhibition of GSK-3β induced the formation of multiple axon-like neurites in hippocampal neurons. The expression of constitutively active GSK-3β impaired neuronal polarization, whereas the nonphosphorylated form of CRMP-2 counteracted the inhibitory effects of GSK-3β, indicating that GSK-3β regulates neuronal polarity through the phosphorylation of CRMP-2. Treatment of hippocampal neurons with neurotrophin-3 (NT-3) induced inactivation of GSK-3β and dephosphorylation of CRMP-2. Knockdown of CRMP-2 inhibited NT-3-induced axon outgrowth. These results suggest that NT-3 decreases phosphorylated CRMP-2 and increases nonphosphorylated active CRMP-2, thereby promoting axon outgrowth.

Introduction

The neuron is one of the most highly polarized cells known and is comprised of two structurally and functionally distinct parts, an axon and dendrites (Craig and Banker, 1994). The specification of the axon is thought to depend on its length relative to the other minor processes, which are called immature neurites (Bradke and Dotti, 2000). Elongation of one of the immature neurites is necessary for axon specification. Intracellular mechanisms that help to enhance neurite/axon outgrowth evidently require reorganization of cytoskeletons including actin filaments and microtubules. Microtubule assembly occurs in the cell body and the growth cone (Brown et al., 1992). Formation of the microtubule array in the neurite/axon is generated by two mechanisms: the transport of microtubule polymer and the microtubule assembly at the plus ends of the microtubules. Both appear to contribute to axon outgrowth (Baas, 1997).

CRMP-2, which also has been independently identified as Ulip2/CRMP-62/TOAD-64/DRP-2, is one of at least five isoforms (Goshima et al., 1995; Arimura et al., 2004). CRMP-2 is expressed exclusively and highly in the developing nervous system. Mutations in the UNC-33 gene, a *Caenorhabditis elegans* homolog of CRMPs, lead to severely uncoordinated movement and abnormalities in the guidance of axons of many neurons (Hedgecock et al., 1985). Previously, we showed that CRMP-2 is enriched in the growing axon of hippocampal neurons, the overexpression of full-length CRMP-2 induces the formation of multiple axons and elongation of the primary axon, and the dominant-negative form of CRMP-2 inhibits axon formation (Inagaki et al., 2001). CRMP-2 shows the ability to convert immature neurites and preexisting dendrites to axons. Thus, CRMP-2 is crucial for axon outgrowth and determination of the fate of the axon and dendrites, thereby establishing and maintaining neuronal polarity. In addition, we recently demonstrated that CRMP-2 binds to tubulin heterodimers to promote microtubule assembly, thereby enhancing axon elongation and branching (Fukata et al., 2002). However, the molecular mechanism by which CRMP-2 is regulated remains unclear.

A ternary complex of PAR-3, PAR-6, and atypical protein kinase C (aPKC) functions in various cell polarization events from worms to mammals (Etienne-Manneville and Hall, 2003b), including cultured hippocampal neurons (Shi et al., 2003; Nishimura et al., 2004). The PAR-6-PAR-3-aPKC complex accumulates at the tip of the axon, and its polarized localization and aPKC activity are important for axon specification (Shi et al., 2003; Nishimura et al., 2004). aPKC can also phosphorylate GSK-3β and inactivate its kinase activity, and GSK-3β is important for polarization of migrating fibroblasts (Etienne-Manneville and Hall, 2003a). However, it remains unknown whether GSK-3β is involved in neuronal polarity and, if so, what the target substrates of GSK-3β are.

We report here that GSK-3β phosphorylates CRMP-2 at Thr-514, inactivates the CRMP-2 activity, and participates in neuronal polarization through CRMP-2. NT-3 and brain-derived neurotrophic factor (BDNF) inhibit GSK-3β via the phosphatidylinositol-3-kinase (PI3-kinase)/Akt (also known as PKB) pathway, and thereby reduce phosphorylation levels of CRMP-2 at Thr-514, leading to axon elongation and branching.

Results

GSK-3β Phosphorylates CRMP-2

It has been previously reported that the phosphorylation of CRMP-2 at Thr-514 by unidentified kinases induces the mobility shift of CRMP-2 (Gu et al., 2000). The optimal consensus site for the phosphorylation by GSK-3β is

*Correspondence: kaibuchi@med.nagoya-u.ac.jp

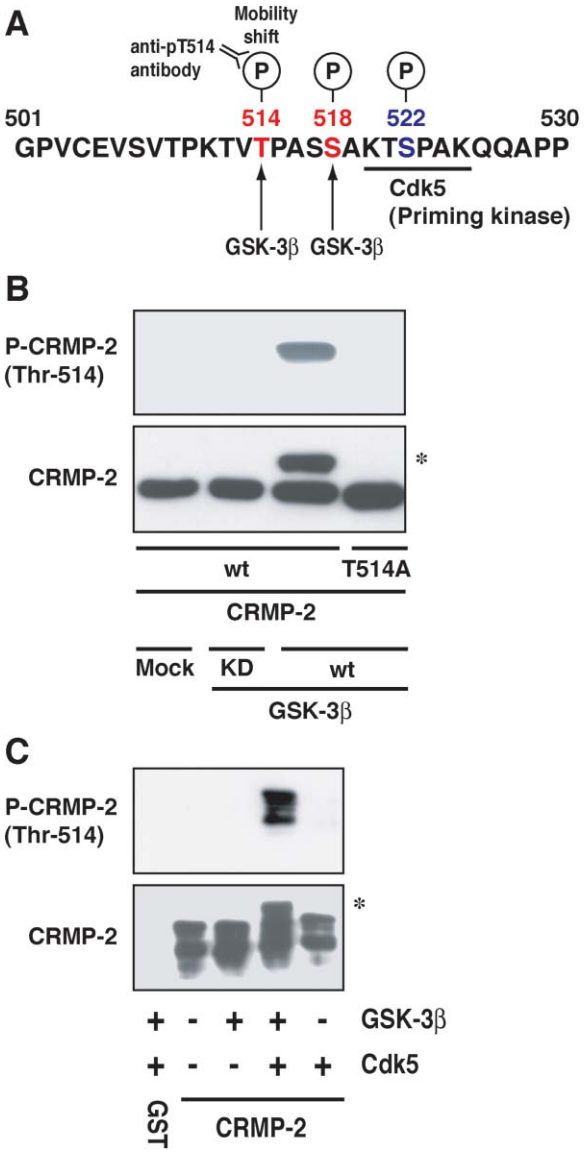

Figure 1. GSK-3β Phosphorylates CRMP-2 at Thr-514

(A) Potential phosphorylation sites of CRMP-2 by GSK-3β and Cdk5. The numbers denote amino acid positions. The optimal consensus site for the phosphorylation by GSK-3β is Ser/Thr-Xaa-Xaa-Xaa-Ser/Thr (where Xaa represents any amino acid). The black bar shows a consensus motif recognized by Cdk5.

(B) COS7 cells were cotransfected with CRMP-2 and GSK-3β mutants. Samples were subjected to immunoblot analysis with anti-pT514 (top) and anti-CRMP-2 (bottom) antibodies. The mobility shift of CRMP-2 (asterisk) was caused by the phosphorylation of CRMP-2 at Thr-514.

(C) Kinase assay was performed using purified CRMP-2, GSK-3β, and Cdk5 in vitro. Each reaction mixture was subjected to SDS-PAGE and immunoblot analysis with anti-pT514 (top) and anti-CRMP-2 (bottom) antibodies.

Ser/Thr-Xaa-Xaa-Xaa-Ser/Thr (where Xaa represents any amino acid; Frame and Cohen [2001]; Eldar-Finkelman [2002]). Considering the consensus sequences of GSK-3β, we speculated that CRMP-2 was phosphorylated by GSK-3β at Thr-514 (Figure 1A). To examine whether GSK-3β phosphorylates CRMP-2, COS7 cells were cotransfected with GSK-3β wild-type (wt) and CRMP-2 wt and subjected to immunoblot analysis with anti-CRMP-2 antibody (Figure 1B). The mobility shift of CRMP-2 (asterisk) was observed in the cells cotransfected with GSK-3β wt and CRMP-2 wt. We then produced the antibody that specifically recognized phosphorylated CRMP-2 at Thr-514 (anti-pT514 antibody). In the COS7 cells cotransfected with CRMP-2 wt and GSK-3β wt, anti-pT514 antibody recognized the upper bands, which corresponded to the phosphorylated CRMP-2 at Thr-514. In contrast, the immunoreactive band was not observed in runs with CRMP-2 T514A (Thr-514 was replaced by Ala) and GSK-3β wt. Consistent with the result using anti-pT514 antibody, the mobility shift of CRMP-2 (asterisk) was not observed in these cells. These results suggest that GSK-3β phosphorylates CRMP-2 at Thr-514.

Next, we examined whether GSK-3β phosphorylates CRMP-2 at Thr-514 in vitro (Figure 1C). The phosphorylation of CRMP-2 at Thr-514 was not observed when GSK-3β alone was added. GSK-3β requires prephosphorylation of its substrate (Eldar-Finkelman, 2002). CRMP-2 has a consensus motif recognized by Cdk5 at Ser-522 in the vicinity of the phosphorylation site of GSK-3β, Thr-514. We found that GSK-3β phosphorylated CRMP-2 that was prephosphorylated by Cdk5 in vitro. When Cdk5 alone was added, CRMP-2 at Thr-514 was not phosphorylated. These results indicate that GSK-3β can phosphorylate CRMP-2 at Thr-514 after CRMP-2 is phosphorylated by Cdk5.

We then evaluated each phosphorylation site (Thr-514, Ser-518, and Ser-522). Not only CRMP-2 T514A but also S518A (Ser-518 was replaced by Ala), S522A (Ser-522 was replaced by Ala), and AAA (Thr-514, Ser-518, and Ser-522 were replaced by Ala) blocked the band shift of CRMP-2 (see Supplemental Figure S1A at http://www.cell.com/cgi/content/full/120/1/137/DC1/). Consistently, the band immunoreactive with anti-pT514 antibody was not observed in runs with T514A, S518A, S522A, and AAA. It is reported that the phosphorylation of CRMP-2 at Thr-514 but not Ser-518 or Ser-522 induces the mobility shift of CRMP-2 (Gu et al., 2000). These results suggest that Ser-518 and Ser-522 are required for the phosphorylation of CRMP-2 at Thr-514 by GSK-3β. Ser-522 appears to be phosphorylated by Cdk5 as a priming kinase, and Ser-518 and Thr-514 seem to be phosphorylated by GSK-3β after the phosphorylation at Ser-522.

Nonphosphorylated Pool of CRMP-2 Localizes in Axonal Growth Cone

In cultured hippocampal neurons, neurons extend several minor processes during the first 12–24 hr after plating (stages 1 and 2; Dotti et al. [1988]). Then, one of the processes begins to extend rapidly to form an axon, resulting in the morphological polarization of the neuron (stage 3). The remaining processes result in the morphological features of dendrites (stage 4). By 7 days in vitro (DIV), the neurons become highly polarized, and the axon and dendrites continue to mature and subsequently develop (stage 5).

We examined whether CRMP-2 is phosphorylated by GSK-3β in hippocampal neurons during axon outgrowth.

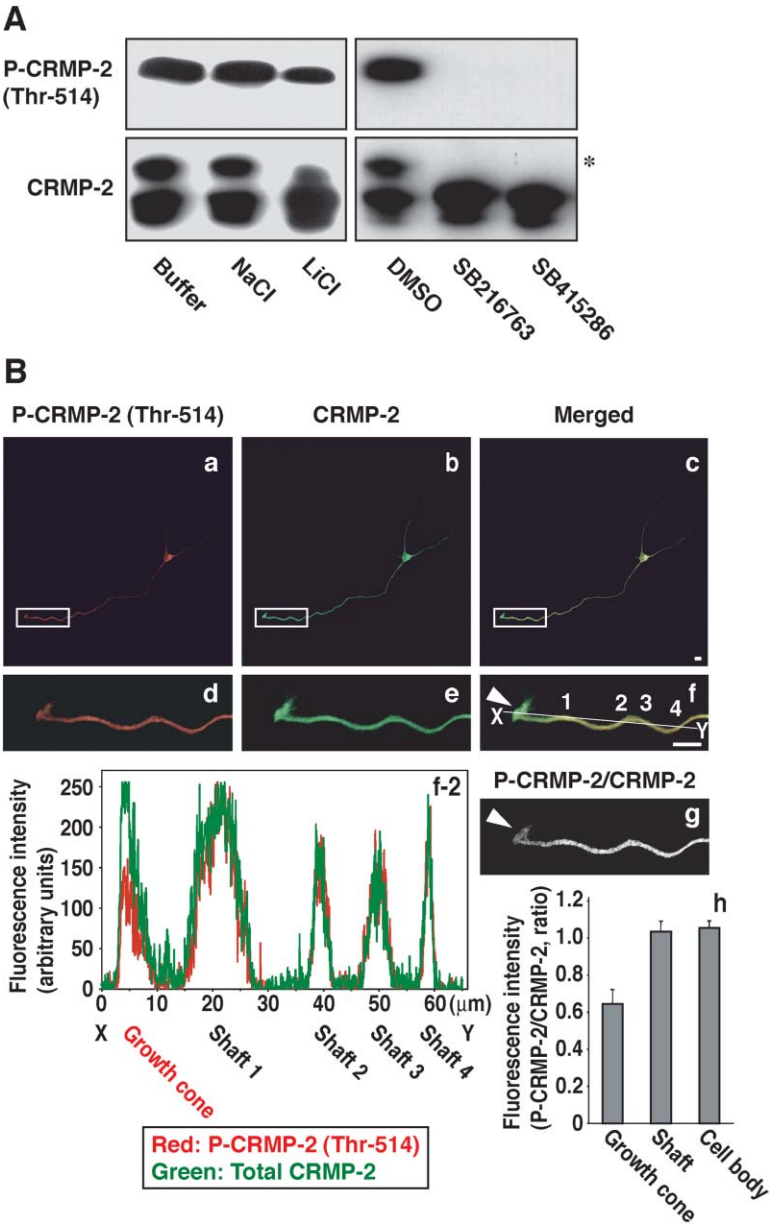

Figure 2. Nonphosphorylated CRMP-2 Localized in the Axonal Growth Cone

(A) Hippocampal neurons were cultured in the presence of GSK-3 inhibitors (2 mM LiCl, 5 μM SB216763, or 25 μM SB415286), buffer, 2 mM NaCl, or DMSO for 48 hr before TCA treatment. Each sample was subjected to SDS-PAGE and immunoblot analysis with anti-pT514 (top) and anti-CRMP-2 (bottom) antibodies. The asterisk indicates the mobility shift of CRMP-2. These results are representative of three independent experiments. (B) Nonphosphorylated pool of CRMP-2 localized in growth cone of growing axon. Hippocampal neurons were fixed at 3 DIV and then immunostained with anti-pT514 (Ba and Bd) and anti-CRMP-2 (Bb and Be) antibodies. The merged (Bc and Bf) and ratio (phosphorylated CRMP-2 to total CRMP-2, [Bg]) are shown. The graph (Bf-2) plots the fluorescence intensities of CRMP-2 phosphorylated at Thr-514 (red) and total CRMP-2 (green) in the line (Bf, from X to Y). The ratio of fluorescence intensities (phosphorylated CRMP-2 to total CRMP-2) was measured in the indicated areas of 30 cells (arbitrary units per pixel [Bh]). Scale bar, 10 μm.

The immunoblot analysis with anti-pT514 antibody revealed that CRMP-2 was phosphorylated at Thr-514 in hippocampal neurons at 3 DIV (more than 75% of neurons at stage 3; Figure 2A). About 30% of CRMP-2 was constitutively phosphorylated at Thr-514. When hippocampal neurons were cultured in the presence of GSK-3 inhibitors (LiCl, SB216763, or SB415286), the phosphorylation levels of CRMP-2 at Thr-514 were decreased. Cdk inhibitor (olomoucine) also decreased the phosphorylation levels of CRMP-2 at Thr-514 (see Supplemental Figure S1B on the *Cell* web site). These results suggest that GSK-3β phosphorylates CRMP-2 at Thr-514 after CRMP-2 is phosphorylated by Cdk5 in hippocampal neurons.

To investigate the spatial distribution of phosphorylated CRMP-2 at Thr-514, hippocampal neurons were fixed at 3 DIV and then immunostained with anti-pT514 (phosphorylated CRMP-2, red) and anti-CRMP-2 antibodies (total CRMP-2, green; Figure 2B). CRMP-2 (green) was enriched in the distal part of the growing axon as previously reported (Inagaki et al., 2001). Phosphorylated CRMP-2 at Thr-514 (red) was enriched in the distal part of the growing axon without growth cone. The merged images of CRMP-2 and phosphorylated CRMP-2 at Thr-514 immunofluorescence enable us to roughly estimate the phosphorylation levels of CRMP-2. The merged image in the shaft was yellow, whereas that in the axonal growth cone was more greenish than that in the shaft. Thus, the ratio of phosphorylated CRMP-2 to total CRMP-2 in the axonal growth cone was lower than that in the shaft.

Further, clear evidence was obtained by intensity imaging of phosphorylated CRMP-2 and total CRMP-2 (Figure 2B). The intensity imaging was similar in shafts,

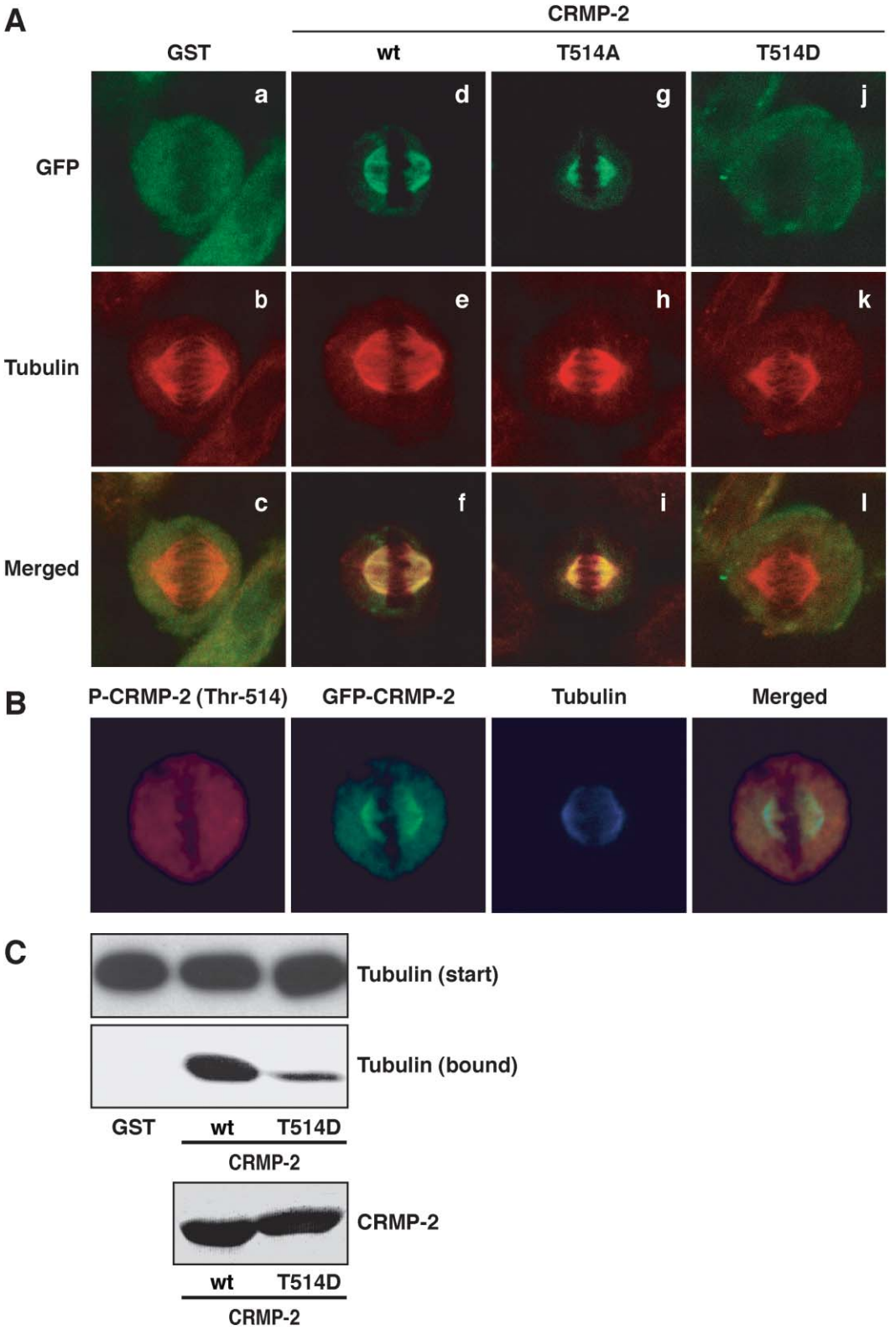

Figure 3. Phosphorylated CRMP-2 Lowers Its Activity to Interact with Tubulin

(A) HeLa cells were transfected with GFP-GST (Aa–Ac), GFP-CRMP-2 wt (Ad–Af), T514A (Ag–Ai), or T514D (Aj–Al). They were then immunostained with anti-tubulin antibody (DM1A; [Ab], [Ae], [Ah], and [Ak]). HeLa cells having spindles in mitotic phase were chosen to show the CRMP-2 localization.

(B) HeLa cells transfected with GFP-CRMP-2 wt were immunostained with anti-pT514 and tubulin (DM1A) antibodies.

(C) Porcine brain lysate was mixed with glutathione-Sepharose 4B beads coated with purified GST, CRMP-2 wt-GST, or CRMP-2 T514D-

whereas that of phosphorylated CRMP-2 was lower than that of total CRMP-2 in the axonal growth cone. The intensity of total CRMP-2 and phosphorylated CRMP-2 in the dendrites were lower than those in the axon. These results indicate that there is a nonphosphorylated CRMP-2 pool at Thr-514 in the growing axonal growth cone. We confirmed that GSK-3 inhibitor decreased the phosphorylation levels of CRMP-2 by immunostaining with anti-pT514 antibody (Supplemental Figure S1C).

Phosphorylation of CRMP-2 Lowers its Activity for Interaction with Tubulin

We recently found that the phosphorylation of CRMP-2 at Thr-555 by Rho-kinase turns off the ability of CRMP-2 to bind tubulin (N. Arimura, C. Menager, Y.K., Y. Fukata, M. Amano, Y. Goshima, N. Morone, J. Usukura, and K.K., unpublished data). Here, we tried to prepare CRMP-2 phosphorylated by GSK-3β in vitro but found that the stoichiometry of the phosphorylation was less than 40%. Then, we produced and characterized a phosphomimic CRMP-2 mutant. CRMP-2 T514D (Thr-514 was replaced by Asp) is expected to mimic the phosphorylated form of CRMP-2 (Kamisoyama et al., 1994; Sweeney et al., 1994; Bresnick et al., 1995). Because ectopic CRMP-2 was diffusely overexpressed in neurons, it was difficult to examine the colocalization of ectopic CRMP-2 with microtubules in detail at axons. Instead, we used HeLa cells, in which green fluorescent protein (GFP)-tagged CRMP-2 was uniformly distributed along microtubules (Fukata et al., 2002). GFP-CRMP-2 wt was clearly localized along the mitotic spindle (N. Arimura, C. Menager, Y.K., Y. Fukata, M. Amano, Y. Goshima, N. Morone, J. Usukura, and K.K., unpublished data; Figure 3A, Supplemental Figure S1D). GFP-CRMP-2 T514A, S518A, S522A, and AAA were also localized along the mitotic spindle, whereas GFP-CRMP-2 T514D, S518D, S522D, and DDD resulted in lower ability to localize along the mitotic spindle (Figure 3A, Supplemental Figure S1D). Under the same conditions, phosphorylated CRMP-2 was diffusely distributed throughout the cytoplasm and not localized along the mitotic spindle (Figure 3B).

Next, we directly compared the binding activity of CRMP-2 wt and T514D to tubulin in vitro. Porcine brain lysate, which contained tubulin, was mixed with glutathione-Sepharose 4B beads coated with GST, CRMP-2 wt-GST, or CRMP-2 T514D-GST. Tubulin bound to CRMP-2 wt-GST as previously described (Fukata et al., 2002; Figure 3C). The stoichiometry of bound tubulin to CRMP-2 wt was about 0.3, whereas the stoichiometry of bound tubulin to CRMP-2 T514D was about 0.05. The binding activity of CRMP-2 T514D to tubulin was weaker than that of CRMP-2 wt. Taken together, these results suggest that the binding activity of CRMP-2 to tubulin is decreased by the phosphorylation of CRMP-2 by GSK-3β.

Nonphosphorylated CRMP-2 Promotes Axon Outgrowth and Induces the Formation of Multiple Axon-Like Neurites

To examine the effect of CRMP-2 mutants, hippocampal neurons were transfected with Myc-CRMP-2 wt, T514A, or T514D and fixed at 3 DIV. CRMP-2 wt enhanced axon elongation and branching as previously reported (Fukata et al., 2002; Figures 4A and 4B). CRMP-2 T514A promoted axon outgrowth and branching more than CRMP-2 wt, whereas CRMP-2 T514D had the weaker activity. These results are consistent with the observation that CRMP-2 T514D showed lower activity to interact with tubulin. CRMP-2 S518A, S522A, and AAA promoted axon outgrowth as well as CRMP-2 T514A (Supplemental Figure S2A).

To examine the effect of CRMP-2 mutants on axon formation, hippocampal neurons transfected with Myc-CRMP-2 wt, T514A, or T514D were fixed at 6 DIV. To visualize secondary axons, neurons at 6 DIV are better than those at 3 DIV because the secondary axons appear later (Inagaki et al., 2001). CRMP-2 wt induced the formation of multiple axon-like neurites as previously reported (Inagaki et al. [2001]; Figure 4D). CRMP-2 T514A increased the percentage of neurons that had multiple long neurites and multiple Tau-1-positive neurites (Figures 4C and 4D). The effect of CRMP-2 T514A on the formation of multiple axon-like neurites was stronger than that of CRMP-2 wt, whereas CRMP-2 T514D showed the weaker activity (Figure 4D). The consistent results were obtained by using other axonal markers, such as synapsin I and synaptophysin for axon and MAP2 for dendrite (Fletcher et al., 1991; Supplemental Figure S2B). CRMP-2 S518A, S522A, and AAA induced the formation of multiple axon-like neurites as well as CRMP-2 T514A (Supplemental Figure S2C).

GSK-3β Regulates Neuronal Polarity via CRMP-2

Inhibition of GSK-3β results in enhanced neurite growth in rat cerebellar granule neurons and DRG neurons (Munoz-Montano et al., 1999; Jones et al., 2003). To investigate the effect of inhibition of GSK-3β on axon outgrowth and formation, hippocampal neurons were cultured in the presence of GSK-3 inhibitors (LiCl, SB216763, or SB415286). These inhibitors slightly enhanced axon elongation (Figure 5A) and branching (data not shown) at 3 DIV and increased the percentage of neurons that had multiple long neurites and multiple Tau-1-positive neurites at 6 DIV (Figures 5B and 5C). The consistent results were obtained by using other axonal markers, such as synapsin I and synaptophysin for axon and MAP2 for dendrite (Supplemental Figure S3A).

To confirm these results, we used hairpin short interfering RNA (siRNA) construct for GSK-3β (Yu et al., 2003). Previous applications of the same hairpin siRNA construct in mammalian cells have shown efficient and specific inhibition of GSK-3β (Yu et al., 2003), and we

GST in vitro. The bound proteins were coeluted with GST fusion proteins by the addition of buffer containing glutathione. Portions of start samples (top) and eluates (middle) were subjected to SDS-PAGE followed by immunoblot analysis with anti-tubulin antibody (DM1A). CRMP-2 wt-GST and CRMP-2 T514D-GST were immobilized in comparable quantities (bottom; Coomassie brilliant blue staining). These results are representative of three independent experiments.

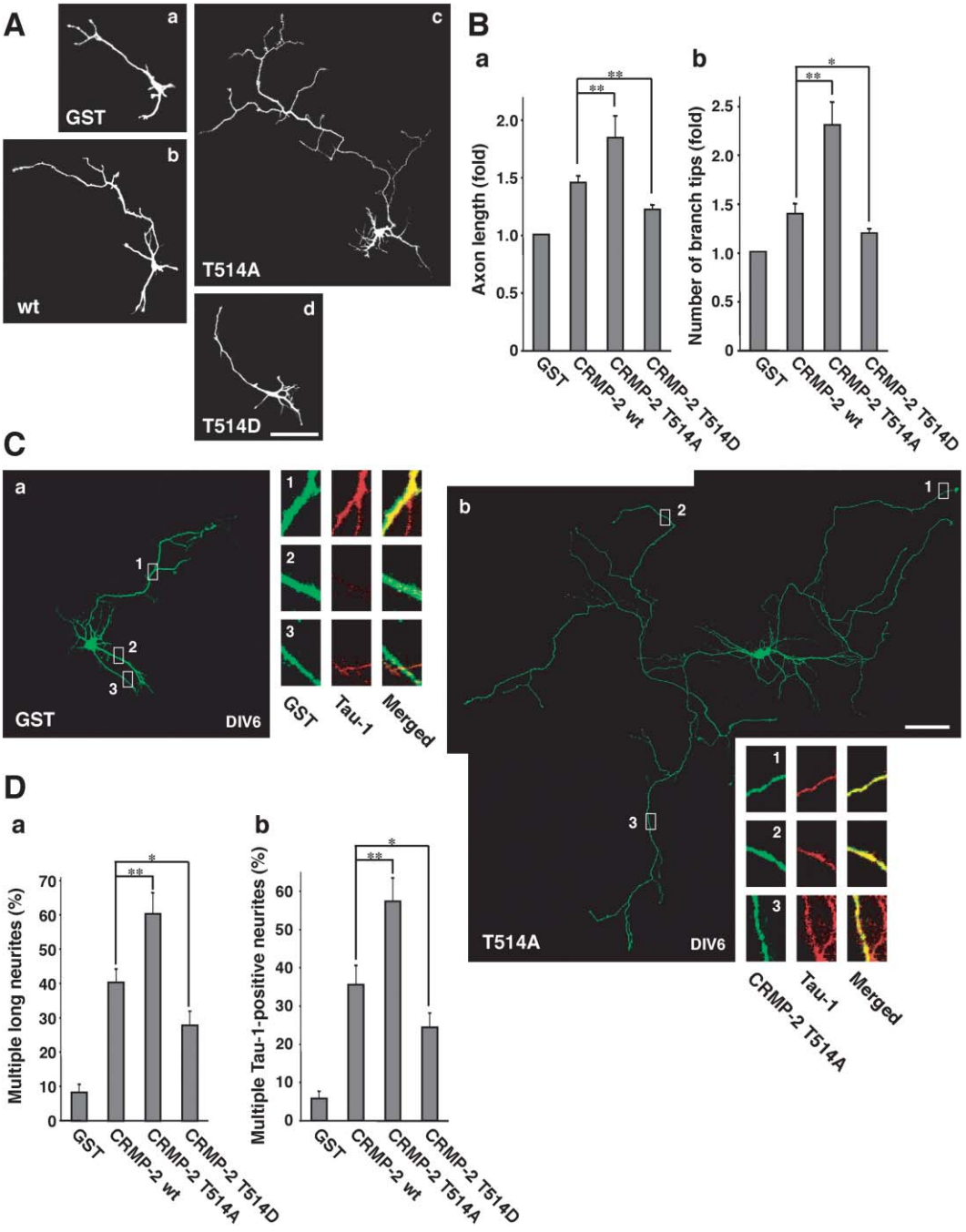

Figure 4. Nonphosphorylated CRMP-2 Enhanced Axon Elongation and Branching and Induced the Formation of Multiple Axon-Like Neurites

(A) Hippocampal neurons were transfected with Myc-GST (Aa), Myc-CRMP-2 wt (Ab), T514A (Ac), or T514D (Ad). Neurons were fixed at 3 DIV and then immunostained with anti-Myc antibody. Scale bar, 100 μm.

(B) Axon length (Ba) and the number of branch tips per axon (Bb) were measured at 3 DIV neurons transfected with the indicated plasmids. n = 50 per experimental condition. Data are means ± SD of triplicate determinations. Asterisks indicate statistical significance (Student's t test; *$p < 0.05$; **$p < 0.01$).

(C) Hippocampal neurons were transfected with Myc-GST (Ca), Myc-CRMP-2 T514A (Cb). Neurons were fixed at 6 DIV and then immunostained with anti-Myc and Tau-1 antibodies. The enlarged images of the neurites (1, 2, 3) are shown. The neuron transfected with Myc-GST (Ca) had one Tau-1-positive neurite (1). The neuron transfected with Myc-CRMP-2 T514A (Cb) had multiple Tau-1-positive neurites (1, 2, 3). Scale bar, 100 μm.

(D) The percentages of the cells that had multiple long neurites (Da) and multiple Tau-1-positive neurites (Db) were measured at 6 DIV neurons transfected with the indicated plasmids. Fifty cells for each plasmid were measured by tracing images of immunofluorescence staining with anti-Myc antibody. Data are means ± SD of triplicate determinations. Asterisks indicate statistical significance (Student's t test; *$p < 0.05$; **$p < 0.01$).

obtained the similar result in rat 3Y1 cells (Supplemental Figure S3B), indicating that the hairpin siRNA construct for GSK-3β is effective in rat cells. Rat hippocampal neurons were cotransfected with hairpin siRNA for GSK-3β and Myc-GST. Inhibition of GSK-3β by hairpin siRNA enhanced axon elongation at 3 DIV (Figure 5A) and increased the percentage of neurons that had multiple long neurites and multiple Tau-1-positive neurites at 6 DIV (Figures 5B and 5C). The consistent results were obtained by using other axonal markers, such as synapsin I and synaptophysin for axon and MAP2 for dendrite (data not shown).

Next, hippocampal neurons were cotransfected with HA-GSK-3β wt, S9A (Ser-9 was replaced by Ala; constitutively active form), or KD (Lys-85 was replaced by Met; kinase dead mutant) and Myc-GST. The ectopic expression of GSK-3β wt and S9A inhibited axon elongation (Figures 5D and 5E) and branching (data not shown) at 3 DIV, whereas GSK-3β KD had no apparent effect. Most of the cells transfected with Myc-GST (about 75%) displayed normal polarity with a single neurite, which was stained with Tau-1 antibody, and some minor processes (Nishimura et al., 2004). The remaining (about 25%) neurons expressing Myc-GST remained in stage 2 of development. The expression of GSK-3β wt and S9A increased the percentage of neurons that have no Tau-1-positive neurites (Figures 5D and 5E). GSK-3β S9A showed slightly higher activity than GSK-3β wt in this capacity. GSK-3β KD had no obvious effect. The consistent results were obtained by using other axonal markers, such as synapsin I and synaptophysin for axon (Supplemental Figure S3C). Further, the effect of GSK-3β S9A on axon formation was examined at 6 DIV, and the consistent results were obtained (Supplemental Figure S3D). These results suggest that the overexpression of GSK-3β impairs neuronal polarity, presumably by suppressing neurite elongation.

Next, we investigated whether the expression of the nonphosphorylated form of CRMP-2 compensates for the GSK-3β-induced defect. The expression of CRMP-2 wt or CRMP-2 T514A counteracted the effects of GSK-3β S9A on axon outgrowth and neuronal polarity (Figure 5F), but CRMP-2 T514D had no obvious effects (data not shown). Taken together, these results suggest that GSK-3β regulates neuronal polarity through the phosphorylation of CRMP-2, though we can not neglect the possibility that GSK-3α is involved in neuronal polarity.

NT-3 and BDNF Regulate CRMP-2 Phosphorylation via the PI3-Kinase/Akt/GSK-3β Pathway

NT-3 and BDNF but not NGF enhance axon elongation and branching in hippocampal neurons (Ip et al., 1993; Morfini et al., 1994; Labelle and Leclerc, 2000). GSK-3β is known to be constitutively active, and its activity can be inhibited by treatment with NT-3 and BDNF (Huang and Reichardt, 2003; Segal, 2003). This inhibitory mechanism is thought to be mediated by the PI3-kinase/Akt pathway (Markus et al., 2002; Huang and Reichardt, 2003; Segal, 2003). Several groups, including ours, reported that PI3-kinase inhibitors inhibited axon elongation (Shi et al., 2003; Menager at al., 2004). PI3-kinase activates Akt by the phosphorylation of Akt at Thr-308 and Ser-473 via phosphatidylinositol-3,4,5-triphosphate (PIP_3) and phosphoinositide-dependent kinase (PDK; Scheid and Woodgett [2001]). Activated Akt phosphorylates GSK-3β at Ser-9 and inactivates its kinase activity (Grimes and Jope, 2001).

We examined whether NT-3 regulates the phosphorylation levels of CRMP-2 (Figure 6A). Hippocampal neurons were stimulated by NT-3 for 3, 10, 30, or 90 min. A decrease of the phosphorylation levels of CRMP-2 was not observed during first 3 min. After the 10 min stimulation, the phosphorylation levels of CRMP-2 were decreased. The decrease was sustained until at least 90 min after the stimulation. BDNF had a similar effect on CRMP-2 phosphorylation (Figure 6B). Treatment with NT-3 and BDNF increased the phosphorylation levels of Akt at Ser-473 and GSK-3β at Ser-9, whereas NGF had no obvious effects on the phosphorylation levels of CRMP-2, GSK-3β, and Akt (Figure 6B). PI3-kinase inhibitor (wortmannin) inhibited NT-3- and BDNF-induced decrements of the phosphorylation levels of CRMP-2 and increments of the phosphorylation levels of GSK-3β and Akt. Because the phosphorylation of GSK-3β at Ser-9 is known to inactivate GSK-3β, our findings suggest that NT-3 and BDNF decrease the phosphorylation levels of CRMP-2 at Thr-514 and increase nonphosphorylated active CRMP-2 via the PI3-kinase/Akt/GSK-3β pathway.

To examine the effect of NT-3 on the spatial distribution of phosphorylated CRMP-2 at Thr-514, hippocampal neurons were fixed at 3 DIV after the treatment of NT-3 for 30 min and then immunostained with anti-pT514 (phosphorylated CRMP-2, red) and anti-CRMP-2 antibodies (total CRMP-2, green; Figure 6C). The phosphorylation levels of CRMP-2 at Thr-514 (red) were decreased not only in the axonal growth cone but also in the shaft as compared with nontreated cells (Figures 2B and 6C). In the cell body, the obvious decrease of the phosphorylation levels of CRMP-2 was not observed.

We then examined whether CRMP-2 is involved in NT-3- and BDNF-induced axon outgrowth and branching. NT-3 and BDNF promoted axon elongation and branching as previously described (Tucker [2002]; Figures 6D and 6E). We used siRNA to directly test whether endogenous CRMP-2 is required for axon elongation and branching by NT-3 and BDNF (Figure 6E). Expression of CRMP-2 was markedly inhibited by CRMP-2 siRNA in 10%–20% cells as revealed by immunocytochemistry as described (Nishimura et al. [2003]; data not shown). Knockdown of CRMP-2 caused a marked inhibition of NT-3- and BDNF-induced axon elongation and branching, indicating that CRMP-2 is necessary for NT-3- and BNDF-induced axon outgrowth and branching. Taken together, these results suggest that NT-3 decreases the phosphorylation levels of CRMP-2 and increases nonphosphorylated active CRMP-2 to promote axon outgrowth and branching.

Discussion

Phosphorylation of CRMP-2 by GSK-3β

In the present study, we found that CRMP-2 was phosphorylated at Thr-514 by GSK-3β in vitro and in vivo (Figures 1B, 1C, 2A, and 2B; Supplemental Figure S1C). GSK-3β alone did not phosphorylate CRMP-2 in vitro

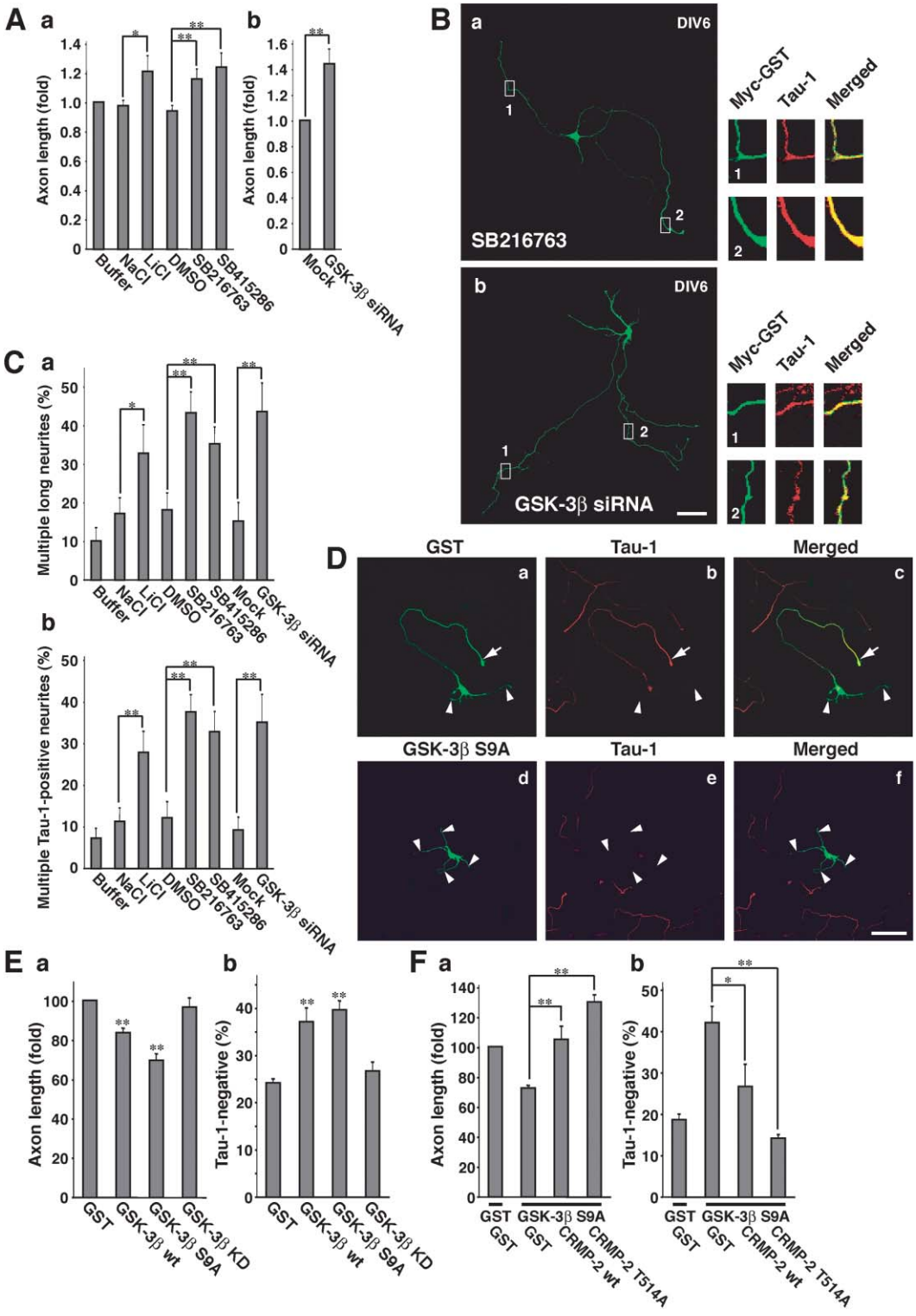

Figure 5. GSK-3β Regulates Neuronal Polarity via CRMP-2

(A) Neurons transfected with Myc-GST were cultured in the presence of GSK-3 inhibitors (2 mM LiCl, 5 μM SB216763 or 25 μM SB415286), buffer, 2 mM NaCl, or DMSO for 48 hr before fixation (Aa). Hairpin siRNA construct for GSK-3β or control vector was cotransfected into neurons with Myc-GST (Ab). Neurons were fixed at 3 DIV and then immunostained with anti-myc antibody to measure axon length. n = 50 per experimental condition. Data are means ± SD of triplicate determinations. Asterisks indicate statistical significance (Student's t test; *$p < 0.05$; **$p < 0.01$).

(B) Neurons transfected with Myc-GST were cultured in the presence of GSK-3 inhibitor (5 μM SB216763) for 5 days before fixation (Ba). Neurons were cotransfected with hairpin siRNA for GSK-3β and Myc-GST (Bb). The neurons were fixed at 6 DIV and then immunostained with anti-Myc and Tau-1 antibodies. The enlarged images of the neurites (1, 2) are shown. The neuron treated with GSK-3 inhibitor (5 μM

(Figure 1C). GSK-3β requires a priming phosphate to phosphorylate its substrates. CRMP-2 has a consensus motif recognized by Cdk5 at Ser-522 in the vicinity of Thr-514 (Figure 1A). We found that treatment of Cdk inhibitor (olomoucine) decreased the phosphorylation levels of CRMP-2 in COS7 cells (data not shown) and hippocampal neurons (Supplemental Figure S1B) and that GSK-3β phosphorylated CRMP-2 that was pre-phosphorylated by Cdk5 in vitro (Figure 1C). Therefore, it is likely that Cdk5 phosphorylates CRMP-2 at Ser-522, whereby GSK-3β phosphorylates CRMP-2 at Thr-514 in vivo. Ser-518 is also a potential phosphorylation site of CRMP-2 by GSK-3β.

Phosphomimic CRMP-2 was not colocalized with the mitotic spindle in vivo (Figure 3A, Supplemental Figure S1D). Phosphorylated CRMP-2 at Thr-514 was not associated with the mitotic spindle (Figure 3B). The binding activity of phosphomimic CRMP-2 to tubulin was weaker than that of CRMP-2 wt in vitro (Figure 3C). These results indicate that the phosphorylation of CRMP-2 at Thr-514 lowers its binding activity to tubulin. Phosphorylated CRMP-2 at Thr-514 was enriched in the growing axon, whereas the phosphorylation levels of CRMP-2 were low in the growth cone (Figure 2B), making it convenient for CRMP-2 to copolymerize with tubulin dimers into microtubules in the growth cone (Arimura et al., 2004). In shafts, the phosphorylation of CRMP-2 at Thr-514 may prevent the copolymerization of CRMP-2 with tubulin dimers into microtubules until reaching the growth cone, or it may induce the dissociation of CRMP-2 from microtubules. It may be noted that the phosphorylation of CRMP-2 at Ser-518 and Ser-522 is implicated in the formation of degenerating neurites in Alzheimer's disease (Gu et al., 2000). Phosphorylated CRMP-2 was identified as an antigen for 3F4 monoclonal antibody, which was raised against partially purified paired helical filaments and labeled neurofibrillary tangles and some plaque neurites. The level of 3F4 antigen is increased in the soluble fraction of the brains affected by Alzheimer's disease. These observations raise the possibility that hyperphosphorylation of CRMP-2 is involved in the development of neurofibrillary tangles and plaque neurites.

Inhibition of GSK-3β prevents semaphorin-3A (Sema3A)-induced growth cone collapse (Eickholt et al., 2002). Uchida et al. (2005) have recently found that Sema3A induces the phosphorylation of CRMP-2 at Ser-522 by Cdk5 followed by the phosphorylation at Thr-509 and Ser-518. Thus, Sema3A appears to increase the phosphorylation levels of CRMP-2 at Ser-522 and thereby promote growth cone collapse.

Neuronal Polarity and GSK-3β

Previously, we found that CRMP-2 is crucial for determining the fate of the axon and dendrites, thereby establishing and maintaining neuronal polarity (Inagaki et al., 2001). CRMP-2 appears to be critical for axon formation by promoting elongation of one of the immature neurites, which is the future axon and within which CRMP-2 is enriched. CRMP-2 binds to tubulin heterodimers and promotes microtubule assembly to enhance axon growth and branching (Fukata et al., 2002). Recently, it has been reported that the polarized distributions of PAR-3/PAR-6 and aPKC activity are important for axon specification in hippocampal neurons and that the PI3-kinase activity at the axon is required for polarized localization of PAR-3 (Shi et al., 2003; Nishimura et al., 2004). We recently reported that the local contact of the immature neurites with adhesion molecules such as laminin induces the rapid production of PIP_3 at the tip of the neurite through the action of PI3-kinase and that PIP_3 is involved in axon specification, possibly by stimulating elongation of an immature neurite (Menager et al., 2004). Elongation of one of the immature neurites is necessary for axon specification (Bradke and Dotti, 2000). The accompanying paper (Jiang et al., 2005 [this issue of *Cell*]) and we have now shown that the expression of constitutively active GSK-3β suppresses axon formation and that inhibition of GSK-3β induces the formation of multiple axons in hippocampal neurons (Figures 5B–5E; Supplemental Figures S3A, S3C, and S3D). We also found that the inhibitory effect of GSK-3β on neuronal polarity is counteracted by nonphosphorylated CRMP-2 (Figure 5F). Taken together, these results indicate that GSK-3β regulates neuronal polarity through the phosphorylation of CRMP-2.

We propose the role of GSK-3β and CRMP-2 in axon specification as follows (Figure 7). The activation of PI3-kinase at the selective immature neurite produces PIP_3, thus activating Akt and recruiting the PAR-3/PAR-6/aPKC complex at the growth cone. Activated Akt and aPKC inhibit GSK-3β by its phosphorylation, whereby nonphosphorylated CRMP-2 is increased in the growth cone. Nonphosphorylated active CRMP-2 promotes microtubule assembly and Numb-mediated endocytosis of cell adhesion molecules to enhance elongation of the immature neurite for axon specification (Fukata et al.,

SB216763) or transfected with hairpin siRNA for GSK-3β had multiple Tau-1-positive neurites (1, 2). Scale bar, 100 μm.

(C) The percentage of the cells that had multiple long neurites (Ca) and multiple Tau-1-positive neurites (Cb) were measured at 6 DIV neurons treated with the indicated compounds or transfected with the indicated plasmids. n = 50 per experimental condition. Data are means ± SD of triplicate determinations. Asterisks indicate statistical significance (Student's t test; *$p < 0.05$; **$p < 0.01$).

(D) Hippocampal neurons were cotransfected with HA-GSK-3β S9A and Myc-GST. Neurons were fixed at 3 DIV and then immunostained with anti-myc (Da and Dd) and axonal marker Tau-1 (Db and De) antibodies. The merged images (Dc and Df) are shown. Arrows indicate Tau-1-positive neurites, and arrowheads denote Tau-1-negative neurites in the transfected cells. Scale bar, 50 μm.

(E) Hippocampal neurons were cotransfected with HA-GSK-3β wt, S9A, or KD and Myc-GST. Neurons were fixed at 3 DIV and then immunostained with anti-myc and axonal marker Tau-1 antibodies. The axon length (Ea) and the percentage of the cells that had no Tau-1-positive neurites (Eb) were measured. Fifty cells for each plasmid were measured by tracing images of immunofluorescence staining with anti-Myc antibody. Data are means ± SD of triplicate determinations. Asterisks indicate statistical significance (Student's t test; **$p < 0.01$).

(F) Cotransfection of HA-GSK-3β wt or S9A with CRMP-2 T514A was performed in hippocampal neurons. The axon length (Fa) and the percentage of the cells that had no Tau-1-positive neurites (Fb) were measured at 3 DIV neurons. n = 50 per experimental condition. Data are means ± SD of triplicate determinations. Asterisks indicate statistical significance (Student's t test; *$p < 0.05$; **$p < 0.01$).

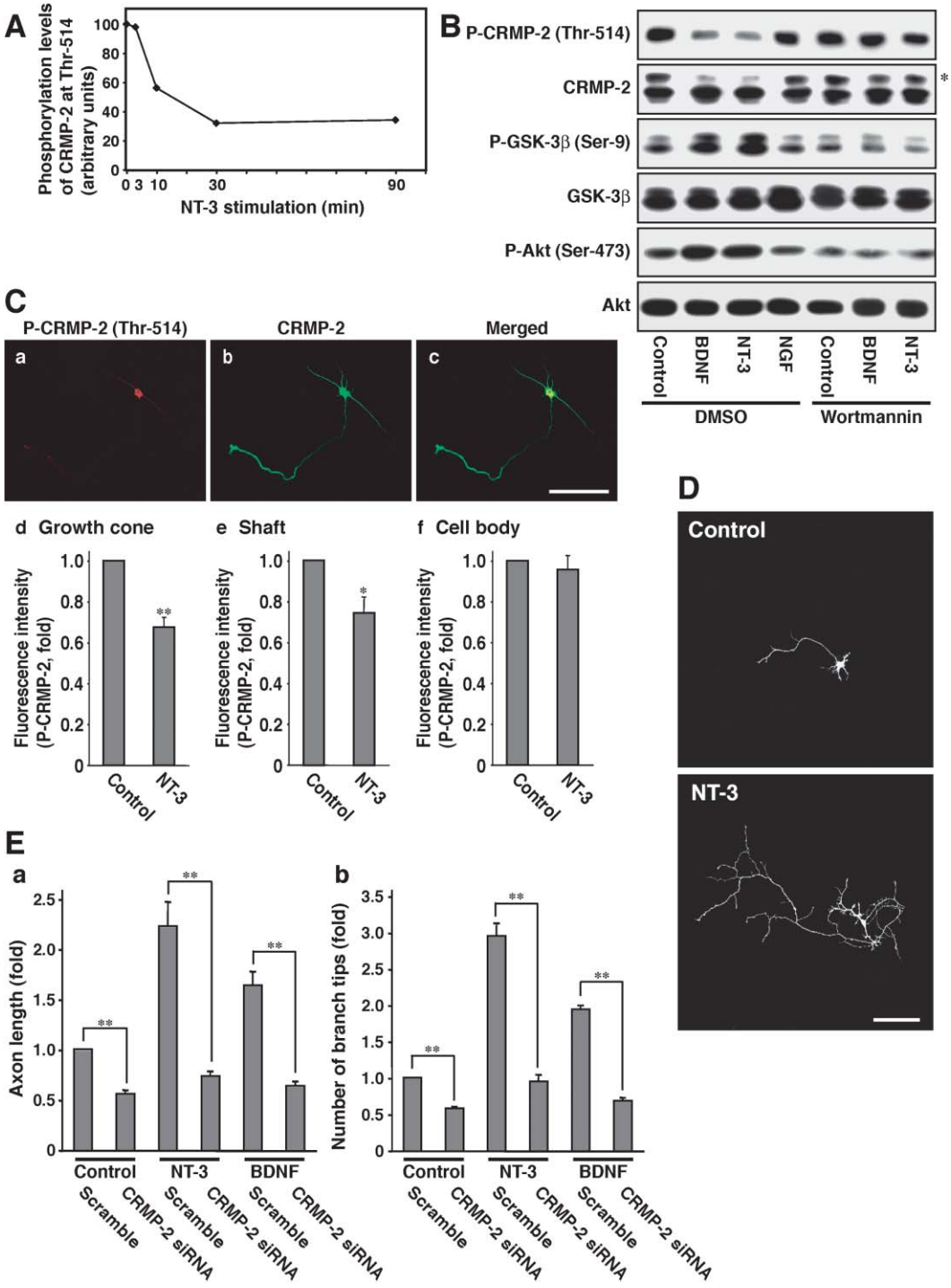

Figure 6. NT-3 and BDNF Regulate CRMP-2 Phosphorylation via the PI3-Kinase/Akt/GSK-3β Pathway

(A) 3 DIV hippocampal neurons were stimulated with NT-3 for 3, 10, 30, or 90 min after neurons were cultured in neurobasal medium for 2 hr. The cell lysates were resolved by SDS-PAGE and immunoblotted with anti-pT514 and anti-CRMP-2 polyclonal antibodies. The relative levels of CRMP-2 phosphorylation at Thr-514 were calculated with those of untreated control cells.

(B) Hippocampal neurons were treated with BDNF, NT-3, or NGF for 30 min after neurons were cultured in neurobasal medium for 2 hr. Neurons were treated with PI3-kinase inhibitor (100 nM wortmannin) or DMSO during the last 2 hr. Immunoblot analyses were performed with anti-pT514, anti-CRMP-2 polyclonal, anti-phospho-GSK-3β (Ser-9), anti-GSK-3β, anti-phospho-Akt (Ser-473), and anti-Akt antibodies. The asterisk shows the mobility shift of CRMP-2 induced by the phosphorylation of CRMP-2 at Thr-514.

(C) NT-3 decreased the phosphorylation levels of CRMP-2 at Thr-514 in the axonal growth cone and the shaft. Hippocampal neurons were fixed at 3 DIV after the treatment of NT-3 for 30 min and then immunostained with anti-pT514 (Ca) and anti-CRMP-2 (Cb) antibodies. The merged (Cc) is shown. The fluorescence intensities of 30 cells were measured in growth cones (Cd), shafts (Ce), and cell bodies (Cf). Scale bar, 50 μm. Data are means ± SD of triplicate determinations. Asterisks indicate statistical significance (Student's t test; *$p < 0.05$; **$p < 0.01$).

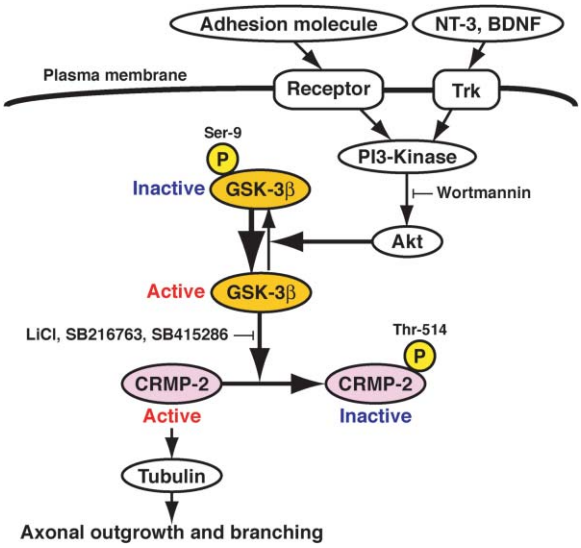

Figure 7. Model Schema to Regulate the Phosphorylation of CRMP-2 by GSK-3β

NT-3, BDNF, and adhesion molecules are thought to activate PI3-kinase, thereby producing PIP_3. PIP_3 activates Akt via PDK. Activated Akt phosphorylates and inactivates GSK-3β. The binding activity of CRMP-2 to tubulin is decreased by the phosphorylation by GSK-3β. Nonphosphorylated CRMP-2 binds to tubulin heterodimers to promote microtubule assembly, thereby enhancing axon elongation and branching.

2002; Nishimura et al., 2003). The relation between Akt and PAR-3/PAR-6/aPKC remains to be clarified.

Inhibition of CRMP-2 Phosphorylation by NT-3 and BDNF

We demonstrated that the phosphorylation of CRMP-2 was suppressed by NT-3 and BDNF (Figures 6A–6C). Knockdown of CRMP-2 with siRNA inhibited NT-3- and BDNF-induced axon outgrowth and branching (Figure 6E). These results suggest that NT-3 and BDNF decrease the phosphorylation levels of CRMP-2 and promote axon outgrowth and branching via nonphosphorylated CRMP-2. NT-3 and BDNF are thought to activate PI3-kinase, thereby producing PIP_3. PIP_3 activates Akt via PDK. Activated Akt phosphorylates and inactivates GSK-3β. Treatment of hippocampal neurons with NT-3 and BDNF resulted in the activation of Akt and the inactivation of GSK-3β (Figure 6B). Activated Akt and inactivated GSK-3β are localized in the growth cone of axons (Eickholt et al., 2002). These findings suggest that NT-3 and BDNF inhibit GSK-3β via the PI3-kinase/Akt pathway, thereby decreasing the phosphorylation levels of CRMP-2 at Thr-514 (Figure 7). It is also possible that NT-3 and BDNF inhibit GSK-3β via the PAR-3/PAR-6/aPKC pathway, and NT-3 and BDNF increase the phosphatase activity toward CRMP-2 to accelerate the dephosphorylation of CRMP-2. Further studies are necessary to address these issues.

One can expect that overdosage of NT-3 or BDNF induces the formation of multiple axons. However, we found that this was not the case. One possible explanation is that NT-3 and BDNF receptors (TrkC and TrkB) may be downregulated or desensitized during the action of NT-3 and BDNF (Frank et al., 1996). Prolonged inhibition of GSK-3β may be necessary for multiple axon formation.

GSK-3β phosphorylates MAP1B and the adenomatous polyposis coil gene product (APC; Grimes and Jope [2001]; Frame and Cohen [2001]). The phosphorylation of MAP1B by GSK-3β suppresses detyrosination of microtubules and decreases the numbers of stable microtubules (Goold et al., 1999; Gordon-Weeks and Fischer, 2000). It is possible that NT-3 and BDNF inhibit GSK-3β and thereby increase the stability of microtubules to enhance axon outgrowth through the dephosphorylation of MAP1B. The binding of APC to microtubules increases microtubule stability, and the interaction of APC with microtubules is decreased by the phosphorylation of APC by GSK-3β (Zumbrunn et al., 2001). Inactivation of GSK-3β by NT-3 and BDNF may induce the interaction of APC with microtubules, thereby stabilizing microtubules. Thus, GSK-3β appears to regulate dynamics of microtubules through the phosphorylation of specific microtubule-associated proteins.

Experimental Procedures

Materials and Chemicals

cDNA encoding human CRMP-2 was obtained using the methods of Arimura et al. (2000). pCAGGS vector was provided by Dr. M. Nakafuku (Cincinnati Children's Hospital Medical Center, Cincinnati, OH). Hairpin siRNA for GSK-3β construct, pU6-GSK-3β HP2, was provided by Dr. David L. Turner (University of Michigan, MI; Yu et al. [2003]). The following antibodies were used: anti-CRMP-2 monoclonal antibody (C4G), kindly provided by Dr. Y. Ihara (University of Tokyo, Tokyo, Japan); anti-CRMP-2 polyclonal antibody raised against MBP-CRMP-2; monoclonal anti-α-tubulin (DM1A, Sigma, St. Louis, MO); monoclonal anti-unique β-tubulin (TUJ1, Berkeley Antibody Company, Richmond, CA); polyclonal anti-c-Myc (A-14, Santa Cruz Biotechnology, Inc., Santa Cruz, CA); anti-GSK-3β (Transduction Laboratories, Lexington, KY); anti-phospho-GSK-3β (Ser-9; Cell Signaling Technology Inc., Beverly, MA); anti-Akt (New England BioLabs, Beverly, MA); anti-phospho-Akt (Ser-473) (New England BioLabs); monoclonal Tau-1 (Chemicon, Temecula, CA); anti-synapsin I (Calbiochem, San Diego, CA); anti-synaptophysin (Chemicon); anti-MAP2 (Sigma); and anti-actin (Chemicon) antibodies. Recombinant human NT-3 and BDNF were purchased from PeproTech EC LTD (London, UK). NGF was from Upstate Biotechnology, Inc. (Charlottesville, VA). Recombinant His-tagged Cdk5 and GST-tagged p35 were from Upstate. GSK-3 inhibitors (SB216763 and SB415286) were from Tocris Cookson, Inc. (Ellisville, MO). Cdk inhibitor (olomoucine) was from Sigma. PI3-kinase inhibitor (wortmannin) was from Wako (Osaka, Japan).

(D) Hippocampal neurons were transfected with Myc-GST and then treated with NT-3 or BDNF. They were fixed at 3 DIV and then immunostained with anti-Myc antibody. Scale bar, 100 μm.

(E) Hippocampal neurons were cotransfected with CRMP-2 siRNA and Myc-GST and then treated with NT-3 or BDNF. They were fixed at 3 DIV and then immunostained with anti-Myc antibody. Axon length (Ea) and the number of branch tips per axon (Eb) were measured at 3 DIV neurons. $n = 50$ per experimental condition. Data are means ± SD of triplicate determinations. Asterisks indicate statistical significance (Student's t test; $^{**}p < 0.01$).

Plasmid Constructs

CRMP-2 mutants were generated with a site-detected mutagenesis kit (Stratagene, La Jolla, CA). The cDNA fragments encoding CRMP-2 wt and mutants were subcloned into pRSET-C1 (Invitrogen, Carlsbad, CA) to obtain the construct of CRMP-2 tagged with histidine (His) at the N terminus of protein, pB-GEX (rearranged vector from pGEX; Amersham Pharmacia Biotech, Buckinghamshire, UK) to obtain the construct of CRMP-2 tagged with GST at the C terminus of protein, pCAGGS-myc, and pEGFP-C1 (Clontech, Palo Alto, CA) vectors, respectively. pCGN-GSK-3β, pCGN-GSK-3β S9A, and pCGN-GSK-3β kinase dead (KD; K85N) and pGEX-2T-GSK-3β were constructed as described by Tanji et al. (2002). All fragments were confirmed by DNA sequencing.

Protein Purification and Preparation of Anti-pT514 Antibody

GST- and His-tagged proteins were purified from *E. coli* on glutathione-Sepharose 4B beads (Amersham) and Ni-NTA agarose (Qiagen, Hilden, Germany) according to the manufacturers' protocols. Rabbit polyclonal antibody against CRMP-2 phosphorylated at Thr-514 (anti-pT514 antibody) was raised as described by Amano et al. (2003). As the antigen, the phosphopeptide Gly-Cys- Thr^{509}-Pro-Lys-Thr-Val-phosphoThr^{514}-Pro-Ala-Ser-Ser-Ala^{519} for CRMP-2 was chemically synthesized by Biologica Co. (Aichi, Japan). The antiserum obtained was then affinity purified against the respective phosphopeptide.

Culture of COS7 and Rat 3Y1 Cells for Immunoblot Analysis

COS7 and rat 3Y1 cells were seeded on a 60 mm dish in Dulbecco's modified Eagle's medium (DMEM) with 10% fetal bovine serum (FBS) and cultured overnight at 37°C in an air/5% CO_2 atmosphere at constant humidity. Transfections were carried out using lipofectamine reagent (Invitrogen) according to the manufacturer's protocol. Cells were grown in DMEM with 10% FBS for 1 day and then in DMEM for 1 day. Cells were treated with 10% (w/v) trichloroacetic acid (TCA). The resulting precipitates were subjected to SDS-PAGE and immunoblot analysis.

Culture of HeLa Cells for Immunofluorescence Analysis

HeLa cells were seeded on coverslips in DMEM with 10% FBS and cultured overnight at 37°C in an air/5% CO_2 atmosphere at constant humidity. Transfections were carried out using lipofectamine reagent. After 2 days' culture, HeLa cells were fixed with 3.7% formaldehyde in phosphate-buffered saline (PBS) for 10 min at room temperature followed by treatment for 10 min with 0.2% Triton X-100 on ice and 10% normal goat serum (NGS) in PBS for 1 hr at room temperature.

Kinase Assay

The kinase reaction for GST-GSK-3β was carried out in 50 μl of kinase buffer (50 mM Tris-HCl [pH 7.5], 0.7 mM EDTA, 12 mM $MgCl_2$, 1 mM dithiothreitol, 100 nM calyculin A) containing 200 μM ATP, recombinant kinases (4.7 μM GST-GSK-3β; 66 nM His-tagged Cdk5 with GST-tagged p35), and substrates (12 μM His-tagged CRMP-2). After incubation for 1 hr at 30°C, the reaction mixtures were boiled in SDS sample buffer and subjected to SDS-PAGE and immunoblot analysis.

In Vitro Binding Assay

GST alone, CRMP-2 wt-GST, or CRMP-2 T514D-GST was separately immobilized onto glutathione-Sepharose 4B beads (Amersham). The immobilized beads were incubated with porcine brain lysate in buffer A (20 mM Tris-HCl, 1 mM EDTA, 50 mM NaCl, 1 mM dithiothreitol, 0.1% NP-40 [pH 7.5]) for 1 hr at 4°C. The beads were washed six times with buffer A containing 150 mM NaCl, and the proteins bound to the washed beads were eluted by the addition of buffer A containing 10 mM glutathione.

Culture of Hippocampal Neurons

Culture of hippocampal neurons prepared from E18 rat embryos using papain was performed as described by Inagaki et al. (2001). Neurons were seeded on coverslips or dishes with poly-D-lysine (PDL; Sigma) and laminin (Iwaki, Tokyo, Japan) for 3 DIV to estimate axon length and branching in neurobasal medium (Invitrogen) supplemented with B-27 supplement (Invitrogen) and 1 mM glutamine. Neurons were seeded on coverslips with PDL only for 6 DIV to visualize secondary axons. Neurons were transfected using a calcium phosphate method before plating to analyze the morphology (Nishimura et al., 2003; Menager et al., 2004). Neurons were fixed at 3 DIV or 6 DIV with 3.7% formaldehyde in PBS for 10 min at room temperature, followed by treatment for 10 min with 0.05% Triton X-100 on ice and 10% NGS in PBS for 1 hr at room temperature. Neurons were then immunostained with indicated antibodies and observed with a confocal laser microscope (LSM510 Carl Zeiss, Oberkochen, Germany) built around an Axiovert 100 M (Carl Zeiss). The length of a longest neurite was measured as that of an axon at 3 DIV. The percentage of neurons with the second longest neurite whose length was longer than a half-length of the longest neurite was counted as that of multiple long neurites. Neurotrophins were added to the medium at a concentration of 100 ng/ml after the transfection. Neurons were cultured for 2 days and were then grown with fresh neurotrophins (100 ng/ml) for 1 day. For some experiments, neurons were treated with 10% (w/v) TCA. The resulting precipitates were subjected to SDS-PAGE and immunoblot analysis.

Acknowledgments

We thank Drs. Y. Ihara (University of Tokyo, Tokyo, Japan) and David L. Turner (University of Michigan, MI) for their kind gifts of materials; Drs. Y. Rao (Washington University, MO), Y. Goshima (Yokohama City University, Kanagawa, Japan), M. Amano, M. Fukata, Y. Fukata, S. Taya, C. Menager, T. Nishimura, Miss K. Fujii, and Mr. A. Hattori for helpful discussion; Miss K. Yamada for preparing some materials and technical assistance; and Mrs. T. Ishii for secretarial assistance. This research was supported in part by grants-in-aid for scientific research from the Ministry of Education, Culture, Sports, Science and Technology of Japan (MEXT); grant-in-aid for Creative Scientific Research from MEXT; The 21st Century Centre of Excellence (COE) Program from MEXT; special coordination funds for promoting Science and Technology (SCFPST); and the Pharmaceuticals and Medical Devices Agency (PMDA).

Received: April 12, 2004
Revised: September 4, 2004
Accepted: November 2, 2004
Published: January 13, 2005

References

Amano, M., Kaneko, T., Maeda, A., Nakayama, M., Ito, M., Yamauchi, T., Goto, H., Fukata, Y., Oshiro, N., Shinohara, A., et al. (2003). Identification of Tau and MAP2 as novel substrates of Rho-kinase and myosin phosphatase. J. Neurochem. *87*, 780–790.

Arimura, N., Inagaki, N., Chihara, K., Menager, C., Nakamura, N., Amano, M., Iwamatsu, A., Goshima, Y., and Kaibuchi, K. (2000). Phosphorylation of collapsin response mediator protein-2 by Rho-kinase: evidence for two separate signaling pathways for growth cone collapse. J. Biol. Chem. *275*, 23973–23980.

Arimura, N., Menager, C., Fukata, Y., and Kaibuchi, K. (2004). Role of CRMP-2 in neuronal polarity. J. Neurobiol. *58*, 34–47.

Baas, P.W. (1997). Microtubules and axonal growth. Curr. Opin. Cell Biol. *9*, 29–36.

Bradke, F., and Dotti, C.G. (2000). Establishment of neuronal polarity: lessons from cultured hippocampal neurons. Curr. Opin. Neurobiol. *10*, 574–581.

Bresnick, A.R., Wolff-Long, V.L., Baumann, O., and Pollard, T.D. (1995). Phosphorylation on threonine-18 of the regulatory light chain dissociates the ATPase and motor properties of smooth muscle myosin II. Biochemistry *34*, 12576–12583.

Brown, A., Slaughter, T., and Black, M.M. (1992). Newly assembled microtubules are concentrated in the proximal and distal regions of growing axons. J. Cell Biol. *119*, 867–882.

Craig, A.M., and Banker, G. (1994). Neuronal polarity. Annu. Rev. Neurosci. *17*, 267–310.

Dotti, C.G., Sullivan, C.A., and Banker, G.A. (1988). The establish-

ment of polarity by hippocampal neurons in culture. J. Neurosci. *8*, 1454–1468.

Eickholt, B.J., Walsh, F.S., and Doherty, P. (2002). An inactive pool of GSK-3 at the leading edge of growth cones is implicated in Semaphorin 3A signaling. J. Cell Biol. *157*, 211–217.

Eldar-Finkelman, H. (2002). Glycogen synthase kinase 3: an emerging therapeutic target. Trends Mol. Med. *8*, 126–132.

Etienne-Manneville, S., and Hall, A. (2003a). Cdc42 regulates GSK-3β and adenomatous polyposis coli to control cell polarity. Nature *421*, 753–756.

Etienne-Manneville, S., and Hall, A. (2003b). Cell polarity: Par6, aPKC and cytoskeletal crosstalk. Curr. Opin. Cell Biol. *15*, 67–72.

Fletcher, T.L., Cameron, P., De Camilli, P., and Banker, G. (1991). The distribution of synapsin I and synaptophysin in hippocampal neurons developing in culture. J. Neurosci. *11*, 1617–1626.

Frame, S., and Cohen, P. (2001). GSK3 takes centre stage more than 20 years after its discovery. Biochem. J. *359*, 1–16.

Frank, L., Ventimiglia, R., Anderson, K., Lindsay, R.M., and Rudge, J.S. (1996). BDNF down-regulates neurotrophin responsiveness, TrkB protein and TrkB mRNA levels in cultured rat hippocampal neurons. Eur. J. Neurosci. *8*, 1220–1230.

Fukata, Y., Itoh, T.J., Kimura, T., Menager, C., Nishimura, T., Shiromizu, T., Watanabe, H., Inagaki, N., Iwamatsu, A., Hotani, H., and Kaibuchi, K. (2002). CRMP-2 binds to tubulin heterodimers to promote microtubule assembly. Nat. Cell Biol. *4*, 583–591.

Goold, R.G., Owen, R., and Gordon-Weeks, P.R. (1999). Glycogen synthase kinase 3β phosphorylation of microtubule-associated protein 1B regulates the stability of microtubules in growth cones. J. Cell Sci. *112*, 3373–3384.

Gordon-Weeks, P.R., and Fischer, I. (2000). MAP1B expression and microtubule stability in growing and regenerating axons. Microsc. Res. Tech. *48*, 63–74.

Goshima, Y., Nakamura, F., Strittmatter, P., and Strittmatter, S.M. (1995). Collapsin-induced growth-cone collapse mediated by an intracellular protein related to UNC-33. Nature *376*, 509–514.

Grimes, C.A., and Jope, R.S. (2001). The multifaceted roles of glycogen synthase kinase 3β in cellular signaling. Prog. Neurobiol. *65*, 391–426.

Gu, Y., Hamajima, N., and Ihara, Y. (2000). Neurofibrillary tangle-associated collapsin response mediator protein-2 (CRMP-2) is highly phosphorylated on Thr-509, Ser-518, and Ser-522. Biochemistry *39*, 4267–4275.

Hedgecock, E.M., Culotti, J.G., Thomson, J.N., and Perkins, L.A. (1985). Axonal guidance mutants of *Caenorhabditis elegans* identified by filling sensory neurons with fluorescein dyes. Dev. Biol. *111*, 158–170.

Huang, E.J., and Reichardt, L.F. (2003). Trk receptors: roles in neuronal signal transduction. Annu. Rev. Biochem. *72*, 609–642.

Inagaki, N., Chihara, K., Arimura, N., Menager, C., Kawano, Y., Matsuo, N., Nishimura, T., Amano, M., and Kaibuchi, K. (2001). CRMP-2 induces axons in cultured hippocampal neurons. Nat. Neurosci. *4*, 781–782.

Ip, N.Y., Li, Y., Yancopoulos, G.D., and Lindsay, R.M. (1993). Cultured hippocampal neurons show responses to BDNF, NT-3, and NT-4, but not NGF. J. Neurosci. *13*, 3394–3405.

Jiang, H., Guo, W., Liang, X., and Rao, Y. (2005). A critical role for glycogen synthase kinase-3β in determining axon-dendrite polarity of neurons. Cell *120*, this issue, 123–135.

Jones, D.M., Tucker, B.A., Rahimtula, M., and Mearow, K.M. (2003). The synergistic effects of NGF and IGF-1 on neurite growth in adult sensory neurons: convergence on the PI 3-kinase signaling pathway. J. Neurochem. *86*, 1116–1128.

Kamisoyama, H., Araki, Y., and Ikebe, M. (1994). Mutagenesis of the phosphorylation site (serine 19) of smooth muscle myosin regulatory light chain and its effects on the properties of myosin. Biochemistry *33*, 840–847.

Labelle, C., and Leclerc, N. (2000). Exogenous BDNF, NT-3 and NT-4 differentially regulate neurite outgrowth in cultured hippocampal neurons. Brain Res. Dev. Brain Res. *123*, 1–11.

Markus, A., Patel, T.D., and Snider, W.D. (2002). Neurotrophic factors and axonal growth. Curr. Opin. Neurobiol. *12*, 523–531.

Menager, C., Arimura, N., Fukata, Y., and Kaibuchi, K. (2004). PIP3 is involved in neuronal polarization and axon formation. J. Neurochem. *89*, 109–118.

Morfini, G., DiTella, M.C., Feiguin, F., Carri, N., and Caceres, A. (1994). Neurotrophin-3 enhances neurite outgrowth in cultured hippocampal pyramidal neurons. J. Neurosci. Res. *39*, 219–232.

Munoz-Montano, J.R., Lim, F., Moreno, F.J., Avila, J., and Diaz-Nido, J. (1999). Glycogen synthase kinase-3 modulates neurite outgrowth in cultured neurons: possible implications for neurite pathology in Alzheimer's disease. J. Alzheimers Dis. *1*, 361–378.

Nishimura, T., Fukata, Y., Kato, K., Yamaguchi, T., Matsuura, Y., Kamiguchi, H., and Kaibuchi, K. (2003). CRMP-2 regulates polarized Numb-mediated endocytosis for axon growth. Nat. Cell Biol. *5*, 819–826.

Nishimura, T., Kato, K., Yamaguchi, T., Fukata, F., Ohno, S., and Kaibuchi, K. (2004). Role of the PAR-3/KIF3 complex in the establishment of neuronal polarity. Nat. Cell Biol. *6*, 328–334.

Scheid, M.P., and Woodgett, J.R. (2001). PKB/AKT: functional insights from genetic models. Nat. Rev. Mol. Cell Biol. *2*, 760–768.

Segal, R.A. (2003). Selectivity in neurotrophin signaling: theme and variations. Annu. Rev. Neurosci. *26*, 299–330.

Shi, S.H., Jan, L.Y., and Jan, Y.N. (2003). Hippocampal neuronal polarity specified by spatially localized mPar3/mPar6 and PI 3-kinase activity. Cell *112*, 63–75.

Sweeney, H.L., Yang, Z., Zhi, G., Stull, J.T., and Trybus, K.M. (1994). Charge replacement near the phosphorylatable serine of the myosin regulatory light chain mimics aspects of phosphorylation. Proc. Natl. Acad. Sci. USA *91*, 1490–1494.

Tanji, C., Yamamoto, H., Yorioka, N., Kohno, N., Kikuchi, K., and Kikuchi, A. (2002). A-kinase anchoring protein AKAP220 binds to glycogen synthase kinase-3β (GSK-3β) and mediates protein kinase A-dependent inhibition of GSK-3β. J. Biol. Chem. *277*, 36955–36961.

Tucker, K.L. (2002). Neurotrophins and the control of axonal outgrowth. Panminerva Med. *44*, 325–333.

Uchida, Y., Ohshima, T., Sasaki, Y., Suzuki, H., Yanai, S., Yamashita, N., Nakamura, F., Takei, K., Ihara, Y., Mikoshiba, K., et al. (2005). Semaphorin-3A signaling is mediated via sequential Cdk5 and GSK3β phosphorylation of CRMP2: implication of common phosphorylating mechanism underlying axon guidance and Alzheimer's disease. Genes Cells, in press.

Yu, J.Y., Taylor, J., DeRuiter, S.L., Vojtek, A.B., and Turner, D.L. (2003). Simultaneous inhibition of GSK3α and GSK3β using hairpin siRNA expression vectors. Mol. Ther. *7*, 228–236.

Zumbrunn, J., Kinoshita, K., Hyman, A.A., and Nathke, I.S. (2001). Binding of the adenomatous polyposis coli protein to microtubules increases microtubule stability and is regulated by GSK3β phosphorylation. Curr. Biol. *11*, 44–49.